Strojniški vestnik - Journal of Mechanical Engineering 57(2011)3, 183-191
DOI:10.5545/sv-jme.2010.169
Paper received: 22.08.2009
Paper accepted: 04.03.2010

Lockin-Interferometry: Principle and Applications in NDE

Philipp Menner - Henry Gerhard - Gerd Busse*
Institute of Polymer Technology (IKT), Non-Destructive Testing (IKT-ZfP), Stuttgart University, Germany

Interferometry is relevant for non-destructive evaluation (NDE) since dimensional changes much smaller than an optical wavelength result in detectable signals. Fringe images obtained with Electronic-Speckle-Pattern-Interferometry (ESPI) or shearography display changes of surface topography between two states of an object, usually using a static load. Usually, hidden defects are found by comparing the observed fringe pattern to the one obtained on an intact reference component and to attribute observed differences to a defect.

Our approach is a periodical object illumination with light that is absorbed in the surface to generate heat and a corresponding modulation of thermal expansion. At the same time fringe images are recorded (either with ESPI or shearography) to give a stack. Subsequently, each image is unwrapped and thereafter the time-dependent content of each pixel is Fourier transformed at the excitation frequency, so the result is local amplitude and phase of the modulated response at this frequency. The phase image displays local delay between excitation and response. This phase change depends on the depth where the defect is located since thermal waves are involved.

In this paper, NDE-examples obtained using this new technique are presented. It is also shown how the achieved improvement as compared to conventional interferometry is up to an order of magnitude.

Keywords: Lockin-ESPI, Lockin-Shearography, defect-selective imaging, interferometric depth profiling

0 INTRODUCTION

Shearography is a speckle-interferometrical method which measures the derivative of object deformation along a certain ("shearing") direction. It compares two different object states by superposition of the speckle pattern of the sample, which is a pattern of bright and dark spots ("speckle") that appear when an optically rough surface is illuminated with coherent light. This pattern is a fingerprint of the surface, i.e. changes of the surface (caused by loading the object) affect the speckle pattern. A comparison of the two speckle pattern gives an image with which local strain changes can be revealed. The object is loaded by mechanical force, by variation of internal or ambient pressure (e.g. of tires, pipes etc.), or by heating of the object surface. The latter can be done easily with spotlights: The light of the lamps is absorbed at the surface, and the induced temperature gradient causes buckling of the object. As defects change the local mechanical properties, they can be detected as a result of the locally changed deformation.

1 METHOD: THEORY AND EXPERIMENTAL SETUP

1.1 Conventional Shearography

The test object is illuminated by coherent laser light which is scattered at the object surface and passes a shearing device (a modified Michelson setup). As one of the mirrors is slightly tilted, a light ray from one point of the object surface is superimposed to the light ray from a neighbor point. The resulting intensity of the superposition of the two light waves depends on their relative phase difference, which changes when the object is deformed. Since two neighbouring points are compared, the measurement does not show the deformation itself, but its derivative in the direction where the mirror is tilted ("shearing direction") [1]. By superposition of the speckle patterns of two different object states (e.g. by

*Corr. Author's Address: Institute of Polymer Technology (IKT), Non-Destructive Testing (IKT-ZfP), Stuttgart University, Pfaffenwaldring 32, 70569 Stuttgart, Germany, gerd.busse@ikt.uni-stuttgart.de

pixelwise subtraction), a fringe pattern that reveals local strain changes appears. By temporal phase shifting, the contrast of the fringe pattern can be improved significantly, and it allows revealing the sign of deformation. Shearography is less sensitive to vibrations than other interferometrical methods (e.g. ESPI) and can therefore be used in industrial environments, but it still cannot distinguish defects lying in different depths, and suffers from detecting the deformation of the whole test object, which can hide defects.

Fig. 1 illustrates the optical setup of shearography.

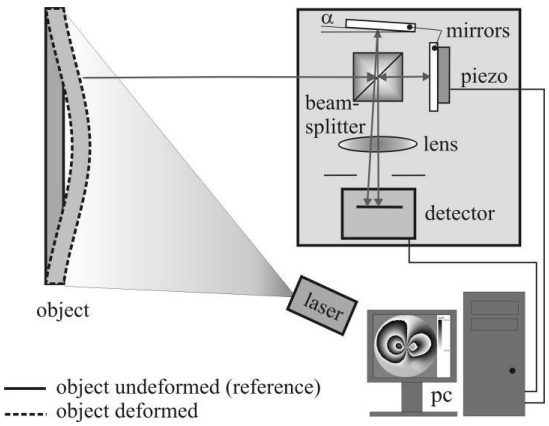

Fig. 1. *Setup of a conventional shearography system*

1.2 Optically Excited Lockin Shearography

Optically excited Lockin shearography is based on the temporal deformation of an object which is illuminated with intensity modulated lamps. Due to absorption of this modulated radiation, the surface temperature changes periodically and drives periodical heat diffusion whose propagation into the interior of the object is described by a "thermal wave". At thermal boundaries, the waves are reflected back to the surface where they are superimposed to the initial thermal wave. In this way, the local phase angle and amplitude of the modulated temperature field change. The defect-induced change of deformation, which is oscillating at the frequency of the lamp modulation, is the effect that is analysed with this method (Fig. 2).

The principle of signal evaluation of an image stack is well known from optically excited Lockin thermography [2] and [3] and could be transferred successfully to the ESPI method [4] and [5] and to shearography [6]. As it was expected from our experience with the other Lockin methods, thermal phase angle images – which do not show the height of an effect, but its local temporal delay with respect to the modulated excitation – are very insensitive to external perturbations. This robustness is based on an internal normalization: the phase angle image results from a Fourier transformation which results in a ratio, so that many artefacts cancel each other. The idea is illustrated by a simplified scheme of a Lockin measurement (Fig. 3).

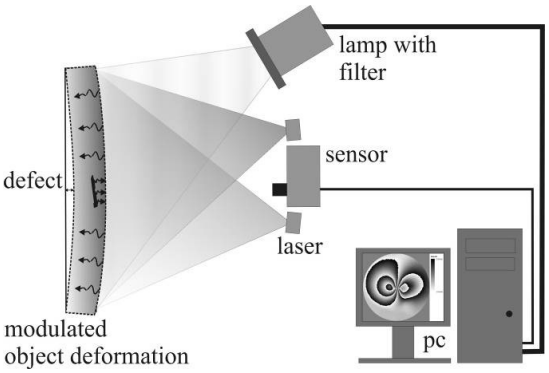

Fig. 2. *Setup of Lockin shearography*

The test object is optically excited by intensity modulated lamps (I) while the camera continuously records images of the speckle pattern of the object surface (II). In order to determine the optical phase distribution, a piezo actuator changes the optical path length of one of the two partial images by $\pi/4$ between the images. A computer calculates optical phase images out of every four speckle pattern images in real time (III). The first optical phase image is used as a reference and is being subtracted from all subsequent optical phase images. This temporal phase shifting results in fringe images with a much higher contrast. In Fig. 3 (III), there are four optical phase images per excitation period. In practice, up to 100 or more can be obtained. A phase unwrapping algorithm converts the fringe pattern into the height profile of the deformation gradient (IV). This stack of demodulated optical phase images contains the information of how the deformation gradient of each pixel changes in time at the modulation frequency (V). To extract this information, the

image stack at each pixel is analyzed for temporal signal changes at the modulation frequency of excitation, while all other changes in the signal are ignored. This filtering is done at each pixel along a vertical column of the image stack ("pixel rod") using a discrete Fourier transformation at the excitation frequency (VI). In this way, the information that is contained in the whole image stack is finally compressed to only two images (VII): the Lockin amplitude image (showing the local height of the modulation effect) and the Lockin phase image, displaying the local thermal phase delay between excitation and object response. It is crucial to distinguish between optical phase images and thermal Lockin phase images: optical phase images are interferometric high-contrast images which are obtained by temporal phase shifting, i.e. by systematic changes of optical path lengths and therewith the phase difference of two light waves. These are the images that the image stack consists of. The Lockin phase image, however, is the result of temporal analysis of the image stack, i.e. it shows the phase angle for each pixel, which corresponds to the local temporal delay of modulated heat flow between excitation and object response. Therefore, this Lockin phase image is the final result, which contains information from the whole image stack.

Fig. 4 illustrates the signal at one pixel both along the time axis and in the frequency domain. The sine modulation of the deformation gradient is seen superimposed to the generally increasing signal, which reaches a plateau towards the end (Fig. 4a). The spectrum of this signal shows two peaks (Fig. 4b). The left peak (at the minimal frequency) is related to the slow warming of the object because the heat that is induced by the lamps cannot be dissipated to the surrounding of the object rapidly enough; it needs some time until a stationary state is reached. The second peak is related to the modulation of the lamps at the excitation ("Lockin") frequency. At this

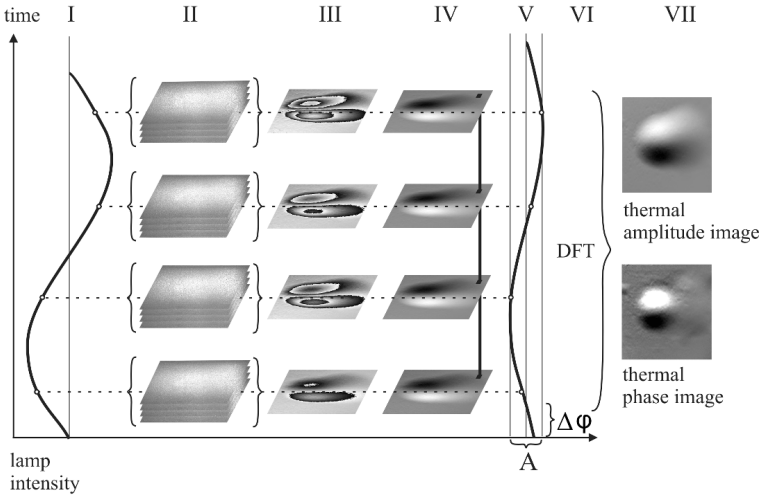

Fig. 3. *Procedure of a Lockin measurement*

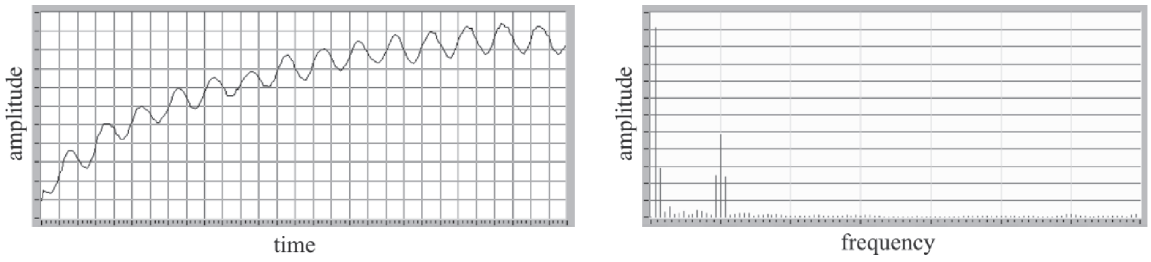

a) *b)*

Fig. 4. *Signal at one pixel rod; a) time domain, b) frequency domain*

frequency, the discrete Fourier transformation is performed. Due to this spectral separation the overall deformation of the object, caused by the slow warming, is eliminated, so that only signal changes matching to the modulation frequency contribute to the phase image.

The excitation frequencies used in this paper are usually below 1 Hz, so the deformation is far away from any mechanical resonance, and there are no inertia effects involved. Therefore, all areas of the object are deforming simultaneously (with a constant temporal delay to the excitation), so the phase angle is constant all over the object, except in case of a defect. The region around the defect is deforming periodically as well, but with a different temporal delay, caused by the reflection of the thermal wave. In this way, defects can be detected very easily, since the intact areas of the object give a constant background, which makes the method defect selective (Fig. 5).

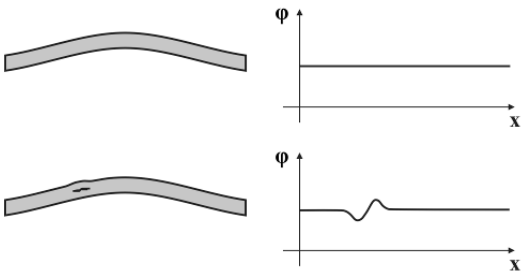

Fig. 5. *Influence of defects on the thermal phase angle under periodical deformation*

Another advantage of Lockin shearography is also directly linked to the use of thermal waves. The thermal diffusion length μ, which is the depth to which the amplitude of the thermal wave has decreased 1/*e* (about 37%), depends on the excitation frequency:

$$\mu = \sqrt{\frac{2\lambda}{\omega \cdot \rho \cdot c_p}}\,, \qquad (1)$$

where λ is thermal conductivity; ρ is density; c_p is specific heat capacity and ω is excitation frequency.

The compression of the image stack to an amplitude- and a phase image via Fourier transformation complies with a weighted averaging, which results in an increased signal-to-noise ratio.

To avoid misunderstanding, it needs to be emphasised that this method differs substantionally from the well-known interferometrical methods used for vibration analysis. While such methods use elastic waves and show vibration nodes, optically excited Lockin Shearography is based on dynamic heat conduction (thermal waves), and at much lower frequencies. It shows local thermal expansion, so the contrast mechanism (the physical principle) is completely different.

1.3 Experimental Setup

For our Lockin shearography system (Fig. 6), a conventional out-of-plane sensor head is used. An array of up to 16 laser diode modules illuminates the sample. The lasers are mounted variably on four arms, so that the object can be illuminated homogeneously, and the sensitivity vector is constant. For thermal excitation, up to four 1 kW spotlights with filters can be used. Disturbances due to convection of warm air are minimized by applying a steady air flow.

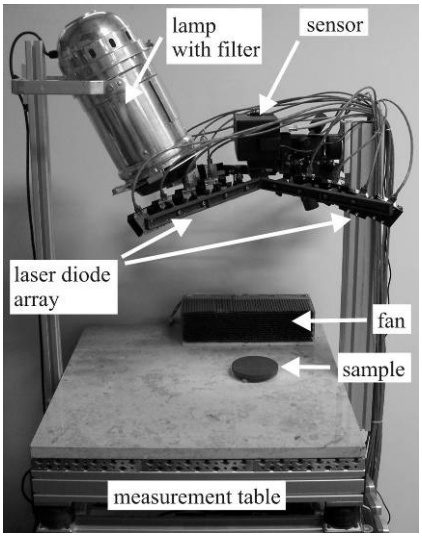

Fig. 6. *Lockin shearography system*

2 RESULTS

2.1 Defect Selectivity

Into a blackened disk of acrylic glass (polymethylmethacrylate, PMMA) with 12 mm in diameter, 16 holes were drilled from the rear

side; the remaining wall thickness ranged from 0.6 to 3.6 mm. After a short and constant excitation of the front side (several seconds), an image sequence was recorded, while the sample cooled down. Fig. 7b illustrates the unwrapped image with the best contrast of the sequence, i.e. this is an optimal conventional shearography image.The top row of the simulated defects is visible well and the row beneath less. The superposed deformation of the whole disk makes the detection of defects more difficult. The same sample was excited periodically at a frequency of 0.05 Hz. Fig. 7c shows the Lockin phase image that was calculated from the sequence. The deformation of the whole disk is eliminated by the Fourier transformation, therefore the holes stand out clearly against the constant background which makes the phase image defect selective (if the sample features a constant thickness). The lowest row can hardly be detected in a phase image at this frequency.

2.2 Signal-to-Noise Ratio

For the determination of the signal-to-noise ration (SNR), another blackened PMMA disk was used containing two pairs of rows of flat bottom holes drilled from the rear side. The pair on the left has a remaining wall thickness of 0.7 mm and the pair on the right 1.4 mm. It was measured at an excitation frequency of 0.04 Hz. The results are illustrated in Fig. 8.

The demodulated conventional image with the best contrast of the sequence (Fig. 8b) displays the left pair of holes and barely the right pair, while the Lockin phase image (Fig. 8c) clearly shows both pairs of hidden holes. The SNR of the image from the sequence is about 3, the SNR of

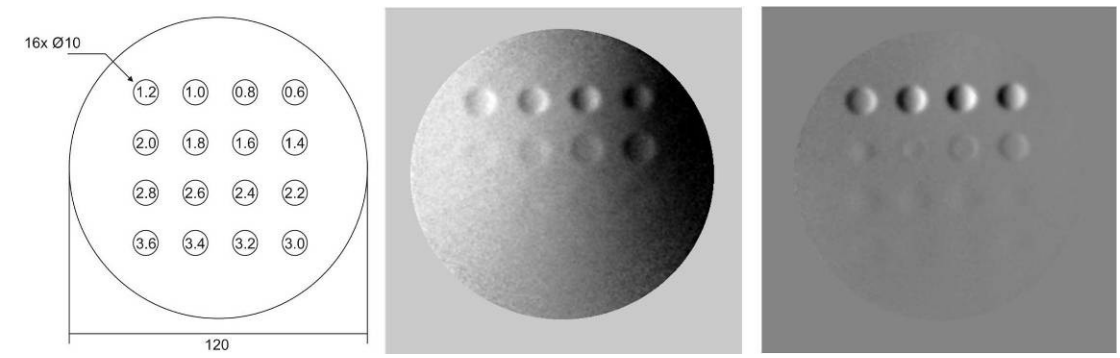

Fig. 7. *a) PMMA sample with simulated defects, b) measured with conventional optically excited shearography, c) Lockin phase image at 0.05 Hz*

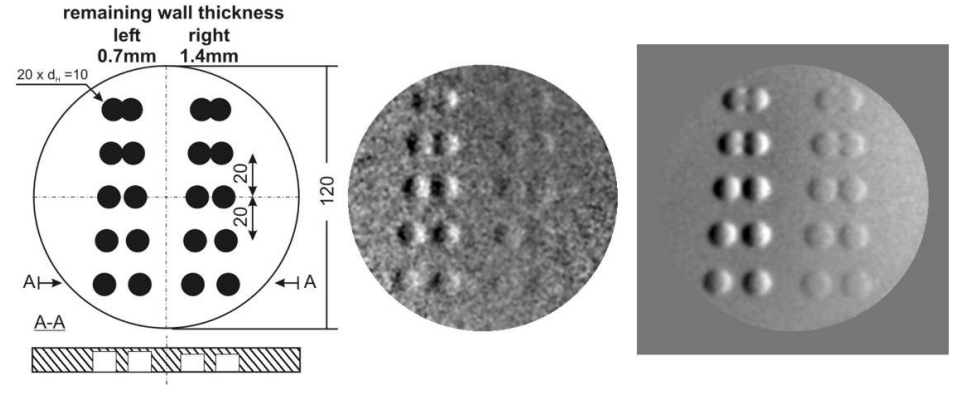

Fig. 8 *a) scheme of PMMA sample, b) best image of Lockin sequence (=conventional result), c) Lockin shearography phase image derived from stack of images*

the Lockin phase is almost 30. Therefore, also the second pair of holes deeper underneath the surface is now clearly seen. The significant improvement by one order of magnitude is based on the phase analysis of the effect coding which is performed by dynamic excitation and the Fourier analysis.

2.3 Depth Resolution

According to Eq. (1), the diffusion length of thermal waves depends on their frequency. Therefore, the thickness of the layer that causes the periodic buckling of an object by its thermal expansion can be adjusted.

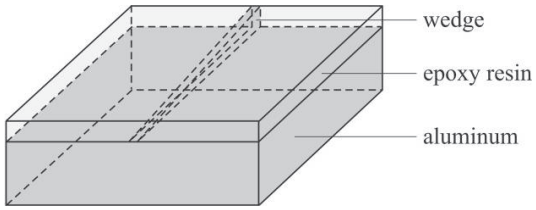

Fig. 9. *Aluminum wedge embedded in epoxy resin*

A series of measurements at various excitation frequencies were taken on an aluminum wedge embedded in epoxy resin (Fig. 9). Therefore, the thickness of the epoxy on top of the aluminum wedge increases continuously

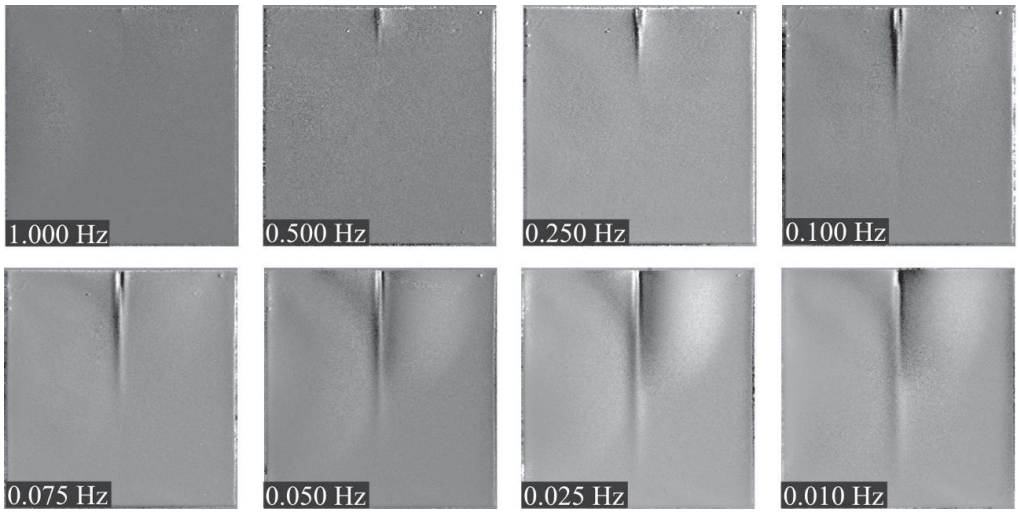

Fig. 10. *Sample of an aluminum wedge embedded in epoxy resin; phase images at various modulation frequencies, measured with optically excited Lockin shearography*

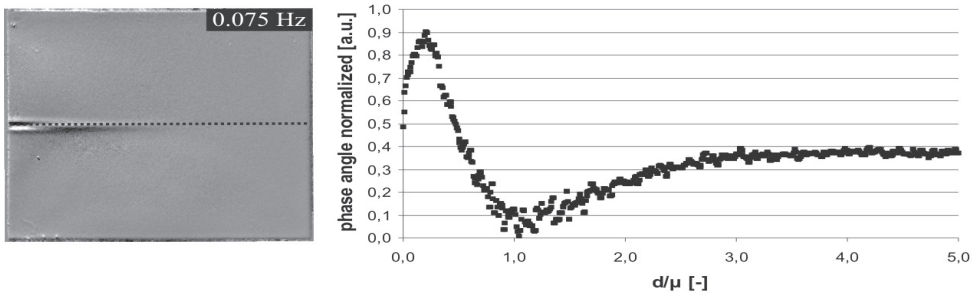

a) *b)*

Fig. 11. *a) Phase image at 0.075 Hz, b) phase angle along dashed line*

along the sample. The results of the measurements are shown in Fig. 10. As the diffusion length of the thermal waves increases with decreasing frequency, more and more of the hidden wedge becomes visible. The point of the phase reversal moves continuously downwards. From 0.05 Hz on, another (unwanted) effect can be observed: during the manufacturing process of the sample two delaminations between the epoxy layer and the aluminum block occurred; one on the left side and one on the right side, next to the wedge. These delaminations can be observed only at lower frequencies (starting from 0.05 Hz) when the diffusion length is large enough.

In Fig. 11, the phase angle at one excitation frequency (here 0.075 Hz) along the dashed line is illustrated in the chart on the right. This kind of curve progression is well-known from Lockin thermography, but while that method is limited to a depth range of about two thermal diffusion lengths, Lockin interferometry provides a larger depth range. In the example shown in Fig. 11, the depth range is about 2.5 the thermal diffusion length, but it may reach values of up to 3.

3 APPLICATIONS

Lockin shearography is well suited to reveal defects which affect the deformation behaviour. This is especially important for components which are safety-relevant, e.g. for aerospace components. Since access to the rear side of components during maintenance is mostly limited, all measurements were performed from the front side. Three typical examples are shown.

3.1 Carbon Fiber Reinforced Plastic Laminate with Impact Damage

A carbon fiber reinforced plastic (CFRP) plate made of multiaxial canvas (Fig. 12a) was damaged with a 5 J impact and inspected with Lockin shearography with an excitation frequency of 0.1 Hz from the impact site.

The best image from the sequence (Fig. 12b) displays only the deformation of the whole plate and there is no indication of the impact. As this deformation of the whole body is eliminated in the Lockin phase image (Fig. 12c), and the SNR enhanced due to the Lockin-method, the impact damage stands out clearly in the middle of this image.

3.2 Debonding in Ultralight Aircraft Wing

The airframe of ultralight aircrafts usually consists of sandwich material like foam core and GFRP cover. Elastic and thermal waves are heavily damped and scattered in such materials, which makes non-destructive testing very difficult. Shearography is a good choice for inspection, as it can reveal defects by monitoring the deformation of the structure under load. Even though thermal waves cannot diffuse deep enough into the structure to reach all defects, Lockin shearography still improves the probability of detection. The Lockin phase image does not show defects located deeply under the surface, but since the amplitude image shows the local modulation height, it can be used to find debondings.

The skin of the wing is bonded at two ribs and at the spar and the leading/trailing edge. Therefore, it deforms periodically in the middle, just like a membrane (though the excitation frequencies are far away from mechanical resonance). The gradient of displacement ranging from black to white should be observable in every field between two fins, the spar and one edge (Fig. 13c, between spar and leading edge). If it ranges over two of these fields, there must be a debonding between a rib and the skin (Fig. 13c, between spar and trailing edge). This can be observed with conventional shearography as well, but since the discrete Fourier transformation works as a weighted averaging, the signal-to-noise-ratio of the Lockin amplitude image is much better.

3.3 Stringer Break in Fuselage Panel of Commuter Airliner

During the development of the Dornier 328, a panel similar to the planned fuselage structure was built to be tested in a buckling mode (Figs. 14a and b).

During the test, a debonding of several stringers occurred. This local debonding can be easily observed in the Lockin phase image (Fig. 14c) in the right, inner part of the panel, since the background signal of the intact area is nearly constant.

4 CONCLUSION

Conventional shearography is a fast and easy method for remote full field non-destructive testing. The combination with the Lockin technique improves shearography significantly: defect selectivity simplifies the interpretation of the results, and the improvement of signal-to-noise ratio by up to one magnitude increases the probability of detection. This reliable method is best applicable to polymer and composite structures since their thermal diffusivity is low and their thermal expansion high.

5 ACKNOWLEDGEMENTS

The authors are grateful to the Institute of Aircraft Design (IFB) of the University of Stuttgart for kindly providing samples, and the Waiblingen aero club for permitting the publication of the results.

6 REFERENCES

[1] Leendertz, J.A., Butters, J.N. (1973). An image-shearing speckle-pattern interferometer for measuring bending moments. *Journal of*

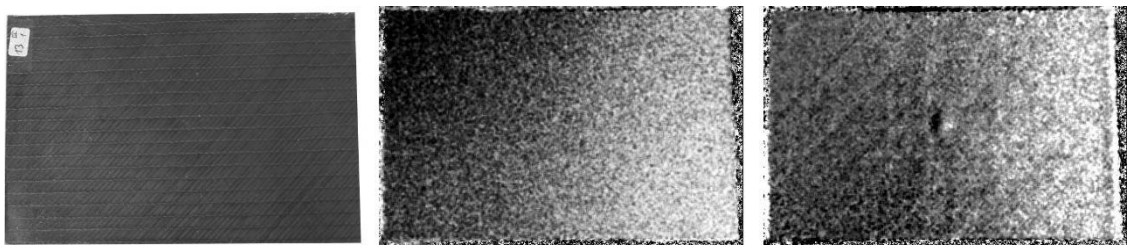

a) *b)* *c)*

Fig. 12. *a) CFRP plate with impact damage, 150 x 100 x 4 mm, b) best image of image sequence, c) Lockin phase image at 0.1 Hz*

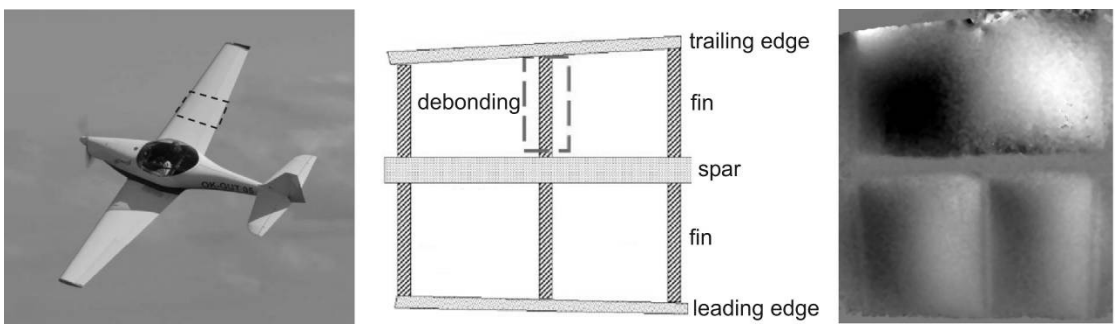

a) *b)* *c)*

Fig. 13. *a) Ultralight aircraft, b) debonding in wing structure, c) Lockin shearography amplitude image at 0.25 Hz*

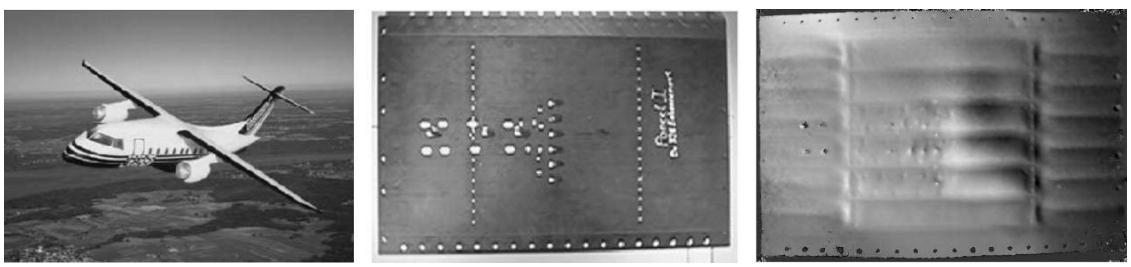

a) *b)* *c)*

Fig. 14. *a) Fairchild Dornier 328, b) CFRP panel used for buckling test, 700 x 1070 x 3.5 mm, c) Lockin phase image at 0.008 Hz*

Physics E: Scientific Instrument 6, p. 1107-1110.

[2] Busse, G. (1992) *Patent no. DE 4203272- C2, 1-3*.

[3] Wu, D. (1996). *Lockin-Thermography for non-destructive material testing and material characterisation*. PhD thesis, University of Stuttgart, p. 24-26. (In German)

[4] Gerhard, H., Busse, G. (2003). Use of ultrasound excitation and optical Lockin method for speckle interferometry deformation measurement. *Proceedings of Nondestructive Characterisation of Materials XI*, Berlin, Springer-Verlag, p. 525-534.

[5] Gerhard, H. (2007). *Development and test of new dynamic speckle methods for non-destructive material and component testing*. PhD thesis, University of Stuttgart, p. 59-61. (In German)

[6] Gerhard, H., Menner, P., Busse, G. (2007). New opportunities and applications of Lockin-Speckle-Interferometry in non-destructive testing of polymers. *Proceedings of Stuttgarter Kunststoff-Kolloquium 20*, 5*V3*, p. 1-8.

[7] Rosencwaig, A., Gersho, A. (1976). Theory of the photo-acoustic effect with solids. *Journal of Applied Physics,* vol. 47, p. 64-69.